Experimental Investigations of Transition Development in Attached Boundary Layers and Laminar Separation Bubbles

W.Würz, S.Wagner
Institut für Aerodynamik und Gasdynamik
Pfaffenwaldring 21, 70550 Stuttgart

Summary

Hot-wire measurements of transitional boundary layer quantities were performed in the Laminar Windtunnel of the IAG under „natural“ conditions on a 2-d airfoil section at a Reynolds number of $Re=1.2*10^6$. The measured amplification of Tollmien-Schlichting waves is compared to linear stability theory. A careful experimental setup allows the measurement of very small velocity fluctuations resulting in a large measurable amplitude ratio of $A_{max}/A_{min}\cong 1800$. The determined „onset“ of transition is compared to the transition prediction with e^n-methods. Some remarks are made on the accuracy of simplified envelope-methods.

Introduction

In the design of airfoils, i.e. for sailplane applications, advantage is gained from long regions of laminar flow. This influences directly the profile drag by means of the lower laminar skin friction in comparison to the turbulent one and indirectly by the possibility of a steeper pressure recovery which can be overcome by a thinner turbulent boundary layer. Transition should occur just before the beginning of the pressure rise to avoid laminar separation bubbles, which may increase the drag significantly. Therefore the resulting performance of a new airfoil depends strongly on the reliability of the method used for transition prediction. Since the fifties various local and non-local empirical methods have been used with more or less success, and today semi-empirical e^n-methods are state of the art [1,2].

Fig.1 shows the lift to drag polar of the SM701 airfoil, originally designed by Somers and Maughmer [3] with the Eppler code [4] which uses a local empirical transition criterion. A re-calculation was made with the airfoil design code XFOIL [5]. This code takes the displacement thickness of the boundary layer into account and predicts the transition by a simplified e^n-method (envelope-method). A large difference to the measured polar [6] can be observed. An attempt was made to adjust the n-factor to the experimental data but resulted also only in poor agreement (and in a very low n-factor, $n\cong 5$). From free-flight experiments performed by Horstman et al. [7]

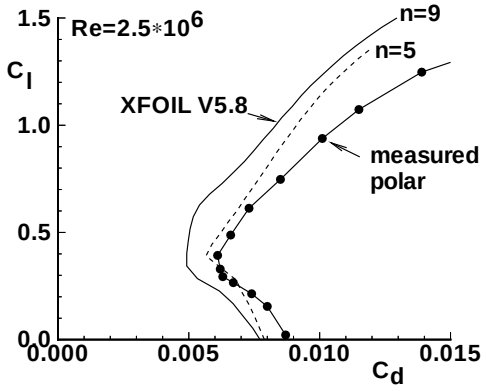

Fig.1: Polar of the SM701 airfoil

n-factors (from linear stability theory calculations) in the range of n≅12-14 are reported, which agree quite well with the corresponding windtunnel data.
To get more insight into this problem, boundary layer measurements were carried out under „natural“ conditions, that means without additional artificial disturbances except the normal windtunnel turbulence. Two cases important for practical applications were examined [8]: transition in an attached boundary-layer under adverse pressure gradient and the transition development in a laminar separation bubble.

Windtunnel and Turbulence level

The Laminar Windtunnel is built as an open return tunnel of the Eiffel design [9]. The rectangular test section measures $0.73*2.73m^2$ and is 3.15m long. The two-dimensional airfoil models span the short distance of the test section. The high contraction ratio of 100:1 and 5 screens and filters result in a very low turbulence level below $2*10^{-4}$.
The turbulence level was measured with a single hot-wire probe DISA55P11 centered in the middle of the test section. The probe was connected to a DISA-55M10 constant temperature anemometer.
The AC part of the signal was cut off by an 20Hz high-pass filter with a roll off rate of 12dB/octave and then amplified with a Preston amplifier. The power spectrum (fig.2) shows the frequency-distribution for a free-stream speed of 30m/s together with the noise-level of the measurement equipment. Above 200Hz the velocity fluctuations can not be distinguished from the electronic noise. Typical Tollmien-Schlichting (TS-) frequencies in the related experiments are in the order of 1kHz. Because of the required high amplification of the signal, the contamination by frequencies from the power consumption (50Hz/100Hz) makes a considerable contribution to the RMS of the signal. These frequencies are digitally filtered out. Then the turbulence level is calculated from the velocity fluctuations in streamwise direction on the assumption of an isotropic turbulence distribution.

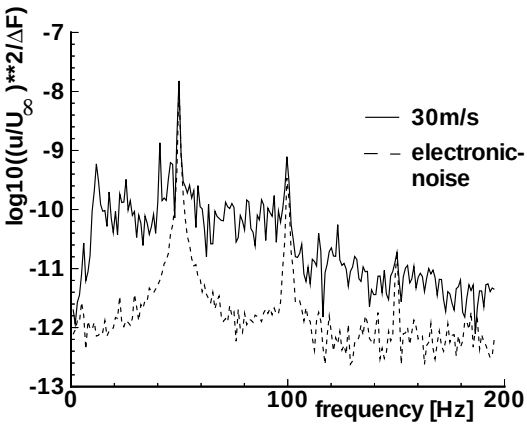

Fig.2: Turbulence spectrum

Instrumentation and Procedure

For the boundary layer measurements a symmetrical airfoil (XIS40MOD) was designed which, depending on the angle of attack, allows the testing of special cases with large differences in boundary layer development and also meets all requirements for the traversing mechanism described below. One side of the airfoil was equipped with 47 pressure orifices (0.3mm diameter), and the pressure distribution was obtained by a scanivalve and a single HBM-PD1 pressure transducer. To avoid any disturbances the other side was smooth and used only for the boundary layer measurements.

A single wire boundary layer probe (DISA55P15) was used for the boundary layer surveys together with a small static pressure probe of 1mm diameter. This probe served as a velocity reference for the hot-wire at the boundary layer edge. The probes are mounted to a small traversing mechanism (fig.3). A thin support resting on the airfoil surface defines its position in relation to the wall. A small rubber between this sting and the airfoil surface prevents the coupling of mechanical vibrations. By means of a high precision rack- and pinion drive together with an optical encoder, a resolution of 5µm in wall distance is achieved. To start traversing a boundary layer, the hot-wire probe is moved towards the wall until its prongs touch a thin graphite coating, thus closing an electric circuit with high impedance which stops the motor. The direction of traverse is reversed and the probe moves until its contact with the wall breaks. By this means, eventual backlash and bending effects are removed. This position is taken as the zero wall distance.

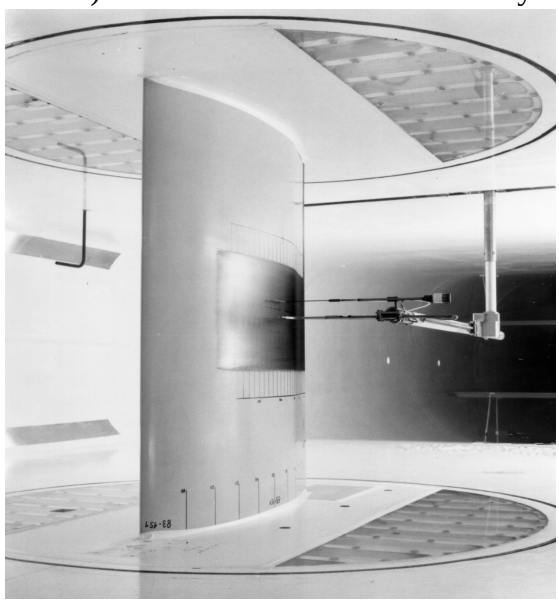

Fig.3: Test section and probe support

Thirty to sixty points are acquired in each boundary layer profile. The DC-output of the hot-wire anemometer is integrated by a low-pass filter at 0.3Hz. The AC-output is high-pass filtered with a special low-noise filter with 570Hz cut-off frequency and a low damping of only 4,3dB/octave. This allows high amplification of the signal in the range of the TS-frequencies by a programmable amplifier and anti-aliasing filter which are remotely controlled by the PC used for data-acquisition. The sampling rate is normally set to 10kHz and the data (4096 time signals) are collected with a 12bit AD-converter. After the FFT analysis the signal is corrected in amplitude to consider the influence of the filters and monitored online.

The calibration of the hot-wire is made according to Kings-Law and is briefly described in [10]. A comparison between the pressure distribution measured with the static probe and those measured with the pressure-orifices shows very good agreement, consequently the influence of the traversing mechanism and probe support on the mean velocity distribution must be small. Only at the rear part of a laminar separation bubble the pressure distributions are slightly diverging, which is probably due to strong curvature of the streamlines which may lead to a misalignment of the static probe.

Boundary layer measurements

Boundary layer measurements were performed for the XIS40MOD airfoil at 1 degree angle of attack and a Reynolds number of $1.2*10^6$ based on the arc-length s_{max}=0.615m measured from the leading edge. The velocity distribution (fig.4) is in good agreement with the distribution calculated with XFOIL. Based on this distribution, the boundary layer parameters are evaluated with a finite difference scheme [11]. The shape factor H_{12} is nearly constant

($H_{12}\cong 2.8$) from $\bar{s}=s/s_{max}=0.25$ to 0.6 and the „onset“ of transition can be clearly seen as the calculated laminar shape factor diverges ($\bar{s}=0.585$) from the measured H_{12}, because the mean velocity profiles are influenced by the increasing turbulence production. Fig.5 shows the measured profiles in comparison to the calculated ones. At each point, a FFT is performed so that eigenfunctions for the TS-frequency can be derived, as plotted in fig.6. These eigenfunctions show a stronger second maximum inside the boundary layer in comparison to 2-d linear stability calculations, also the TS-amplitude ($0.1\%U_\delta$) is distinctly below the critical level for secondary instability effects. Under some assump-tions for the superposition of 2-d and a small amount of oblique travelling waves these eigenfunctions agree satisfactorily with the measured ones.

Under „natural“ conditions, i.e. without a dominating artificial disturbance at one single frequency, it is not clear how to define a TS-amplitude and also a TS-frequency. As can be seen in fig.7, there is a broad band of frequencies which are amplified or damped according to linear theory (if they are small enough). In this study the TS-frequency will be defined as the frequency with the highest measurable amplitude (in the range of amplified frequencies) at the onset of transition. The corresponding TS-amplitude is defined as the maximum amplitude of the eigenfunction (fig.6) for a frequency-range of ±10% of the above mentioned TS-frequency. Normally this covers more than 80% of the energy of the whole amplified frequencies.

In fig.8 the development of the measured TS-amplitudes in the three maxima of the eigenfunction (fig.6) is compared to linear stability theory. A good agreement can be seen, except for $\bar{s}\leq 0.35$. In this region the hot-wire signal is dominated by electronic noise and the influence of probe vibrations. Based on this lowest measurable amplitude A_{min} and the amplitude at the onset of transition A_{tr} ($\bar{s}=0.585$), a high amplitude ratio could be measured, corresponding to an n-factor of n=7.5. The calculation of the n-factor with linear stability theory beginning from the instability point yields n=10.3. The value of this n-factor depends on the definition of the transition point which can be different according to the method used for determining transition. In the present experiment for example the total RMS-maximum of the fluctuation amplitudes is reached at $\bar{s}=0.65$. At the same station the measured wall shear stress increases significantly. For this position the calculated n-factor reaches a value of n=11.5.

A second boundary layer experiment was performed under the same conditions but with an angle of attack of -3 degrees. In this case a laminar separation bubble occurs at $\bar{s}=0.717$ with turbulent reattachment at $\bar{s}=0.82$. The velocity distribution and the development of the integral boundary layer parameters can be seen in fig.9. An additional velocity distribution was measured with a small trip in front of the separation point which causes transition and prevents the formation of the bubble. The influence of the bubble on the velocity distribution is clearly visible. The instability point is at $\bar{s}=0.27$, but according to the low shape factor H_{12} no significant amplification of TS-wave occurs before laminar separation. Inside the bubble, H_{12} grows rapidly and reaches $H_{12max}\cong 6.5$. At $\bar{s}=0.744$ a TS-amplitude of $0.1\%U_\delta$ is observed, which shows that the transition process develops inside the bubble and is therefore dominated by the stability characteristics of the separated shear-layer. Free shear-layers are highly unstable and in the present experiment the

amplification from 0.1% to 3% TS-amplitude took place over a distance of one TS-wavelength ($\lambda_{TS} \cong 0.03\,\bar{s}$). The measured amplification rates are slightly higher inside the bubble in comparison to linear stability calculations. This may be contributed to the parallel flow assumption which is questionable in this case. Nevertheless the calculated n-factor for the onset of transition reaches n=10.5. This is in good agreement with the above mentioned measurement and shows the consistency of this semi-empirical e^n-method.

Transition prediction with envelope-methods

A well known simplification of linear stability calculations for transition prediction are the so-called enevelope-methods. They were first introduced by Gleyzes et al. [12] and later used by Drela in the airfoil design program XFOIL. This method takes advantage from the observation that for a similar boundary layer the amplitude development of different amplified frequencies can be reduced to one envelope covering the amplification curve of all single frequencies (fig.10). This envelope can then be used for the calculation of n-factors. For this purpose, Drela derived an analytic function depending on Falkner-Skan-profiles for the determination of the instability point (1) and a second one for the gradient of the envelope (2). Equation (3) and (4) are derived from the same profiles to enable a direct integration in s.

$$log_{10}(Re_{\delta 2in}) = 2.492\left(1/\left(H_{12}-1\right)\right)^{0.43} + 0.7\left(tanh\left(14.0/\left(H_{12}-1\right)-9.24\right)+1.0\right) \qquad (1)$$

$$dn/d\,Re_{\delta 2} = 0.028\left(H_{12}-1\right) - 0.0345\cdot e^{-\left(3.87/\left(H_{12}-1\right)-2.52\right)^2} \qquad (2)$$

$$m_{H12} = -0.05 + 2.7/\left(H_{12}-1\right) - 5.5/\left(H_{12}-1\right)^2 + 3.0/\left(H_{12}-1\right)^3 \qquad (3)$$

$$dn/ds = m_{H12}\cdot dn/d\,Re_{\delta 2}/\delta_2 \qquad (4)$$

In the vicinity of the instability point a small circular correction is made to the gradient of the envelope-curve to achieve a smooth start.

The key assumption of this method is that the transition development in a boundary layer with non constant shape factor can be described by stepwise integrating along these envelopes. Dini [13] shows that this is not true and results in an „envelope-error“. He analysed a boundary layer development with a sharp increase in the shape factor. In this case, the amplification must be regarded along a single frequency and is usually higher than calculated along the envelope. For example (fig.10), if a boundary layer is stable to all frequencies until Reδ2=200 is reached and then a jump to H_{12}=2.8 occurs in the shape factor, the most amplified single frequency will follow the dotted line. After a short distance, the corresponding „envelope“ is crossed and the n-factor of n=9 is reached further upstream.

In practice, boundary layers develop without sharp jumps in the shape factor and for analysing such a continuous change a special series of boundary layers were calculated (fig.11). An inverse boundary layer method was used to prescribe a linear growth in the shape factor, starting with a flat plate solution. The onset of transition is then calculated according to linear stability theory using fixed single frequencies in comparison with the envelope-method. For a constant shape factor the predicted transition points (n=9) agree quite well. For stronger increase of H_{12}, linear stability theory predicts transition further upstream. The maximum differences in $\bar{s}_{tr}$ are not observed for the strongest

increase in H_{12} because of the higher instability of the boundary layer resulting in a rapid increase in the n-factor with $\bar{s}$.
Fig.12 shows a stability analysis for the above mentioned SM701 airfoil for a lift coefficent of c_l=0.67. The calculated amplitude development for single frequencies is plotted against the corresponding envelope-curve. The experimentally detected transition by a oil and lampblack coating can be seen in fig.13. The increase in wall shear stress caused by the onset of transition results in a bright zone starting at $\bar{s}$=0.4. The lampblack from this zone is transported to the darker zone following downstream. For $\bar{s}$=0.4 a n-factor of n=11.3 can be derived from the linear stability calculations, which is in good agreement with the results from the boundary layer experiments. For the same transition position the envelope-method reaches only n≅6. Since the accuracy of the transition prediction with this method depends strongly on the shape of the boundary layer development, which differs from one airfoil to the other (also for changes in angle of attack, or the upper and lower surface) it is not possible to get consistent n-factors. For practical airfoil design it should also be observed that small changes in the velocity distribution can cause large differences in the transition prediction. A comparison of two slightly different airfoils with this envelope-method may therefore be questionable.

Conclusions

Boundary layer experiments were performed in the Laminar Windtunnel of the IAG using hot-wire anemometry. The measurements were made under „natural“ conditions without introducing a single dominant frequency. According to a careful experimental setup, the development of TS-waves could be studied over a large amplitude range of A_{max}/A_{min}≅1800. The comparison with linear stability theory shows good agreement for the amplified frequency-band and the amplification rates in attached boundary layers, whereas for the laminar separation bubble slightly higher amplification rates were measured. Based on the stability calculations, consistent n-factors for the „onset“ of transition could be derived. It could be shown that the simplified envelope-method leads to an uncertain transition prediction.

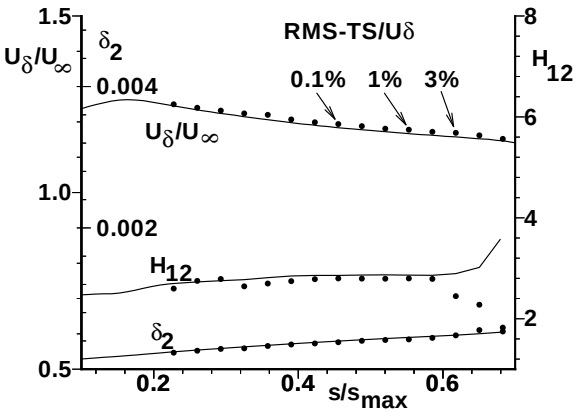

Fig.4: Boundary layer parameters XIS40MOD, α=1°, • experiment

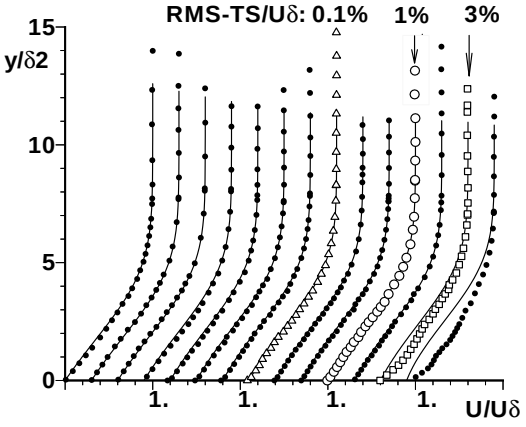

Fig.5: Mean velocity profiles • experiment, — theory [11]

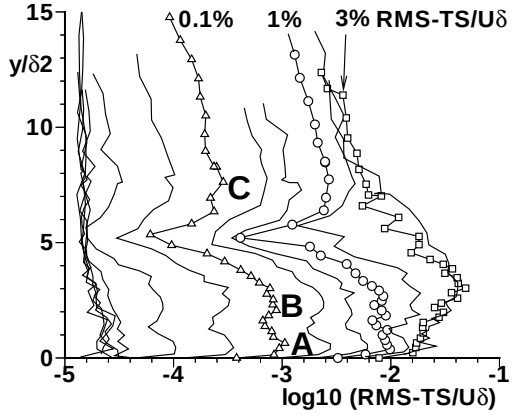

Fig.6: Eigenfunctions for the TS-frequency

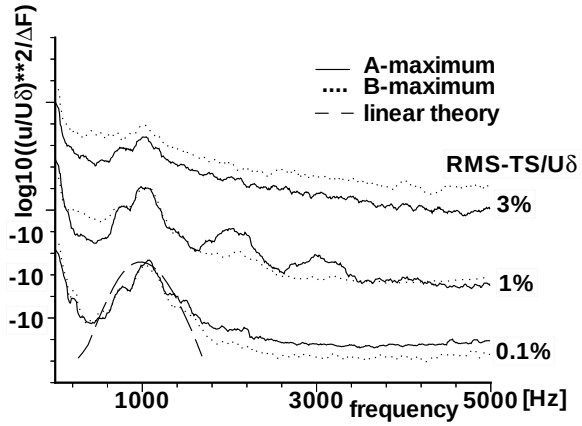

Fig.7: Frequency spectra (shiftet by 2 decades)

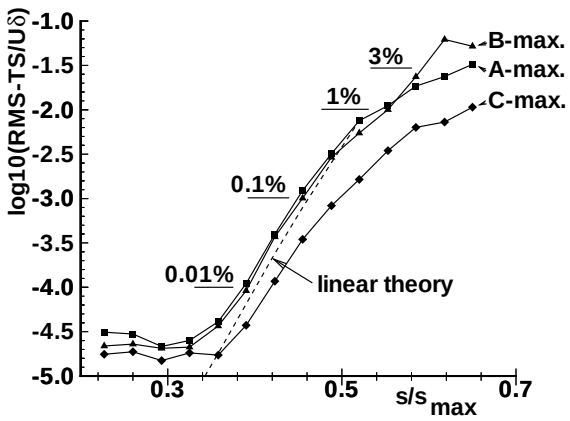

Fig.8: Amplitude development for the TS-frequency

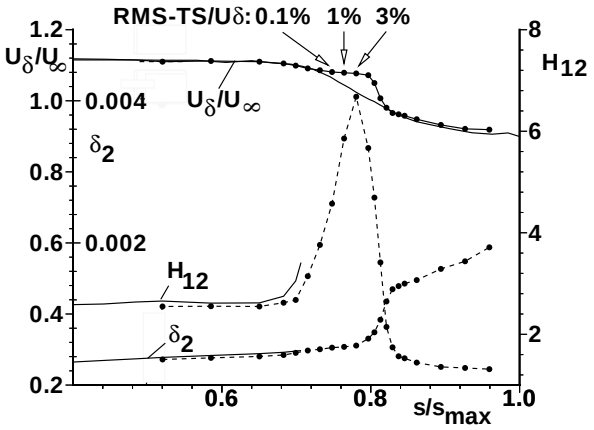

Fig.9: Boundary layer parameters XIS40MOD, α=-3°

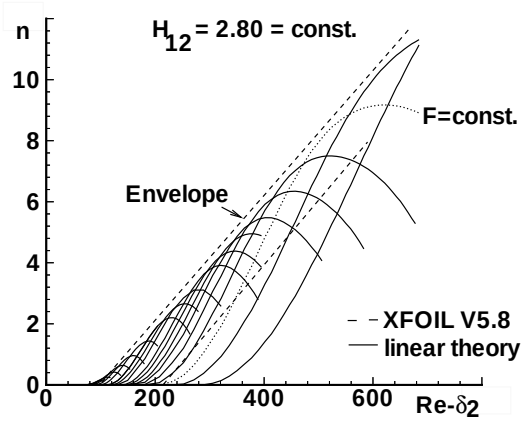

Fig.10: Amplitude development for similar boundary layers

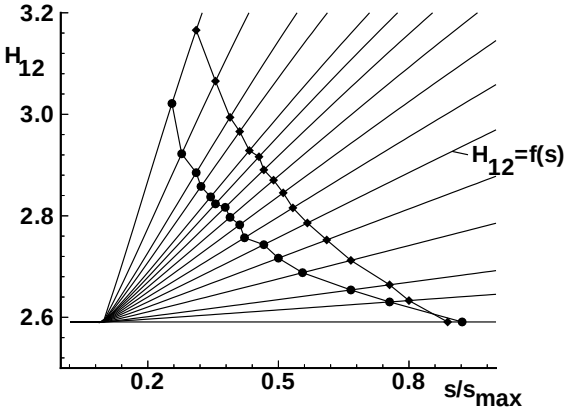

Fig.11: Transition prediction, n=9, • linear theory, ♦ envelope-method

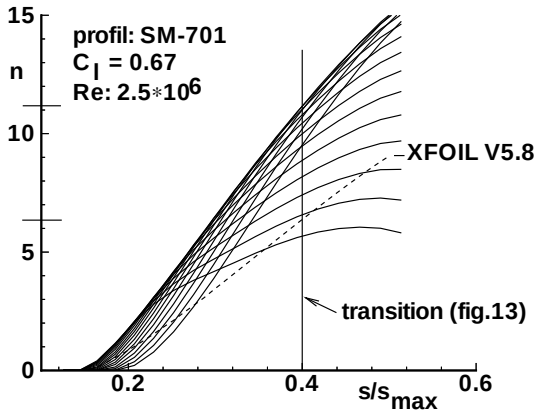

Fig.12: Stability analysis for the SM701 airfoil, - - envelope-curve

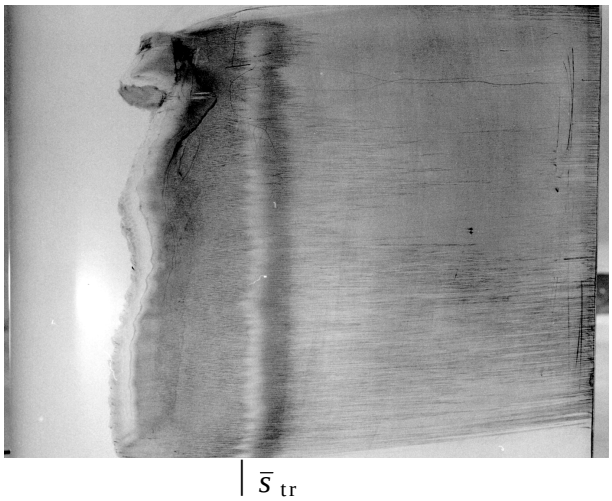

Fig 13: Oil and lampblack coating for transition detection, SM701, flow direction from left to right

References

[1] Arnal,D.: „Description and Prediction of Transition in two-dimensional, incompressible Flow“, AGARD-R-709,pp2.1-2.71 (1984)

[2] Arnal,D.: „Boundary Layer Transition: Prediction, Application to Drag Reduction“, AGARD-R-786, pp5.1-5.59 (1992)

[3] Somers,D.M.; Maughmer,M.D.: „ The SM701 Airfoil: An Airfoil for World Class Sailplanes“, Technical Soaring, Vol.14,No.3 (1992)

[4] Eppler,R.: „Airfoil Design and Data“, Springer Verlag, Berlin-Heidelberg-New York, (1990)

[5] Drela,M.; Giles,M.B.: „Viscous-Inviscid Analysis of Transonic and Low Reynolds Number Airfoils“, AIAA-86-1786-CP (1986)

[6] Althaus,D.; Würz,W.: „Wind Tunnel Tests of the SM701 Airfoil and the UAG88-143/20 Airfoil“, Technical Soaring Vol.17,No.1 (1993)

[7] Horstmann,K.H.; Quast,A.; Redecker,G.: „Flight and Wind-Tunnel Investigations on Boundary-Layer Transition“, Journal of Aircraft, Vol27, No.2, pp146-150 (1989)

[8] Würz,W.: „Hitzdrahtmessungen zum laminar-turbulenten Strömungsumschlag in anliegenden Grenzschichten und Ablöseblasen sowie Vergleich mit der linearen Stabilitätstheorie und empirischen Umschlagskriterien“, Dissertation Universität Stuttgart (1995)

[9] Wortman,F.X.; Althaus,D.: „Der Laminarwindkanal des Instituts für Aerodynamik und Gasdynamik der Technischen Hochschule Stuttgart“ Zeitschrift für Flugwissenschaften, Nr.12, Heft 4

[10] Wubben,F.J.M.: „Experimental Investigation of Tollmien-Schlichting Instability and Transition in Similar Boundary Layer Flow in an Adverse Pressure Gradient (Hartree $\beta = -0.14$)“, TU Delft, Report LR-604 (1991)

[11] Cebeci,T.; Smith,A.M.O.: „Analysis of Turbulent Boundary Layers“, Academic Press, New York (1974)

[12] Gleyzes,C.; Cousteix,J.; Bonnet,J.L.: „Theoretical and Experimental Study of Low Reynolds Number Transitional Separation Bubbles“, Proceedings of the Conference on Low Reynolds Number Airfoil Aerodynamics, UNDAS-CP-77B123, Notre Dame, pp137-151 (1985)

[13] Dini,P.; Selig,M.S.; Maughmer,M.D.: „A simplified e^n-Method for Separated Boundary Layers“, AIAA-91-3285 (1991)